

# Lactate sensing by neuroepithelial cells isolated from the gills of killifish (*Fundulus heteroclitus*)

Erin M. Leonard<sup>1,\*</sup>, Fiona E. Weaver<sup>2</sup>, and Colin A. Nurse<sup>2</sup>

<sup>1</sup>Department of Biology, Wilfred Laurier University, Waterloo, Ontario, N2L 3C5, Canada

<sup>2</sup>Department of Biology, McMaster University, Hamilton, Ontario, L8S 4K1, Canada

\* Author for Correspondence:

Dr. Erin M. Leonard

Department of Biology, Wilfred Laurier University, 75 University Avenue West, Waterloo, Ontario N2L 3C5, Canada

Email: eleonard@wlu.ca

## ABSTRACT

Lactate is produced in most vertebrate cells as a by-product of anaerobic metabolism. In addition to its role as a fuel for many tissues, circulating lactate can act as a signaling molecule and stimulates ventilation in air- and water-breathing vertebrates. Recent evidence suggests lactate acts on O<sub>2</sub>- and CO<sub>2</sub>/H<sup>+</sup>-sensitive chemoreceptors located in the mammalian carotid body. While analogous receptors (neuroepithelial cells or NECs) in fish gills are presumed to also function as lactate sensors, direct evidence is lacking. Here, using ratiometric Fura-2 Ca<sup>2+</sup> imaging, we show that chemosensitive NECs isolated from killifish gills respond to lactate (5-10 mM; pHe ~7.8) with intracellular Ca<sup>2+</sup> elevations. These responses were inhibited by either a L-type Ca<sup>2+</sup> channel blocker (nifedipine; 0.5 μM), a monocarboxylic acid transporter (MCT) blocker (α-cyano-4-hydroxycinnamate; 300 μM), or a competitive MCT substrate (pyruvate; 5 mM). These data provide the first direct evidence that gill NECs act as lactate sensors.

**KEY WORDS: Lactate, O<sub>2</sub>-chemoreceptors, Fish gill, Hypercapnia, L-type Ca<sup>2+</sup> channels, Monocarboxylic acid transporter**

## Summary Statement

Lactate is a metabolic fuel but it also stimulates breathing in vertebrates. We show that in fish this reflex is mediated by gill neuroepithelial cells which act as lactate sensors.

## INTRODUCTION

In many vertebrate cells, lactate is the end product of glycolysis and is used as an energy source by several organs (e.g. heart) following its release and transport via the circulation (Brooks, 2020; Hui et al., 2017). In addition, lactate is now recognized as an important signaling molecule and as a major substrate for gluconeogenesis in the liver (Brooks, 2020). Blood lactate levels increase during systemic hypoxia and physical exercise resulting in several adaptive changes; however, the underlying cellular and molecular mechanisms are not fully understood. For example, in both air- and water-breathing vertebrates circulatory lactate can induce a dose-dependent increase in ventilation, independent of changes in extracellular pH (Chang et al., 2015; Gargaglioni et al., 2003; Hardarson et al., 1998; Thomsen et al., 2019; Thomsen et al., 2017; Torres-Torrelo et al., 2021). In mammals, there is strong evidence that lactate is sensed by  $O_2$  and  $CO_2/H^+$  chemoreceptors (i.e. glomus cells) located in the carotid body (Torres-Torrelo et al., 2021), a major peripheral sensory organ that controls cardiorespiratory reflexes and maintains homeostasis during hypoxemia (Kumar and Prabhakar, 2012). The earlier view that this sensing pathway involves a putative ‘lactate receptor’ (Olf78), that is highly expressed in carotid body glomus cells (Chang et al., 2015), has since been challenged following the demonstration that lactate sensing is preserved in Olf78r-deficient glomus cells (Torres-Torrelo et al., 2021; Torres-Torrelo et al., 2018).

On the other hand, though circulatory lactate stimulates cardiorespiratory reflexes in water-breathers, e.g. teleost fish (catfish and rainbow trout), both the cellular and sub-cellular mechanisms are unknown (Thomsen et al., 2019; Thomsen et al., 2017). Denervation or removal of the first gill arch inhibited lactate sensing in those studies, suggesting a branchial location for the sensors. However, though direct evidence was lacking, the authors presumed lactate sensing was mediated by gill respiratory  $O_2$ ,  $CO_2/H^+$  chemoreceptors, i.e. neuroepithelial cells or NECs (Jonz et al., 2004; Qin et al., 2010), by analogy with carotid body glomus cells and their shared roles in the control of ventilation. In the present study, we directly tested the hypothesis that gill NECs act as lactate sensors by using ratiometric fura-2  $Ca^{2+}$  imaging techniques to monitor intracellular  $Ca^{2+}$  responses during lactate exposure of isolated NECs from the hypoxia tolerant killifish (*Fundulus heteroclitus*). We show that gill NECs possess lactate sensing properties and the signaling pathway shares some of the features recently described for carotid body glomus cells.

## **MATERIALS AND METHODS**

### **Gill cell culture preparation**

Adult killifish (*Fundulus heteroclitus*) of 8-10 g both male and female, kindly supplied by Dr. G. Scott (McMaster University, Hamilton, Ontario), were housed in tanks filled with aerated brackish water at room temperature and maintained as previously described (Borowiec and Scott, 2021). Protocols for animal care were approved by the McMaster University Animal Research Ethics Board. In the experiments described below, killifish were first rendered unconscious by sharp blow to the head followed by decapitation. Dissociated gill cells were obtained using procedures similar to those previously described (Jonz et al., 2004; Zhang et al., 2011). Briefly, gill baskets were removed and rinsed in Leibovitz's media (L-15, Invitrogen, Burlington, ON, Canada) supplemented with 1% penicillin-streptomycin (Sigma–Aldrich, Oakville, ON, Canada), 0.3% glucose and 1% Fetal Bovine Serum (FBS). After mucus removal, isolated gill filaments were enzymatically digested in a 0.5% trypsin/EDTA solution (Sigma-Aldrich, Oakville, Ontario, Canada) for 30 min at room temperature, teased apart with fine forceps, and triturated with a Pasteur pipette. After enzyme inactivation with 10% FBS, the cell suspension was centrifuged, passed through a 70  $\mu\text{m}$  filter, and suspended in L-15 media containing 1% penicillin-streptomycin, 0.3% glucose and 1% FBS. Dissociated gill cells were plated into central wells of modified culture dishes coated with poly L-lysine (0.1 mgml<sup>-1</sup>, Sigma, St Louis, MO, USA) and Matri-Gel (Collaborative Research, Bedford, MA, USA), and incubated for 2-4 hrs at room temperature.

### **Measurements of intracellular calcium**

Cultured gill cells were incubated at 23°C for 30 min in Ringer's solution containing 5  $\mu\text{M}$  Fura-2-AM (Invitrogen). The Ringer's solution contained in (mM): 135 NaCl, 5 KCl, 2 MgCl<sub>2</sub>, 2 CaCl<sub>2</sub>, 10 glucose, 10 Hepes, at pH 7.8. Cultures were washed for 10 min to remove residual Fura-2-AM, and then imaged using a Nikon Eclipse TE2000-U inverted microscope (Nikon, Mississauga, Ontario, Canada) equipped with Lambda DG-4 ultra-high-speed wavelength changer (Sutter Instruments Co., Novato, CA, USA), a Hamamatsu OCRCA-ET digital CCD camera (Hamamatsu, Sewickley, PA, USA) and a Nikon S-Fluor 40x oil-immersion objective lens with a numerical aperture of 1.3. The procedures for data acquisition and analysis were similar to those previously described (Leonard and Nurse, 2020; Zhang et al., 2011). Images

were acquired every 2 s at 340 nm and 380 nm excitation, with an exposure time of 100-200 ms. Ratiometric data were obtained using Simple PCI software version 5.3

### **Histochemistry and Immunofluorescence**

Killifish gill baskets were mounted in paraffin, sectioned at 4  $\mu\text{m}$ , and deparaffinized in xylene and a graded series of ethanol. Sections were stained for H&E or processed for immunofluorescence. Antigen retrieval was obtained using a sodium citrate buffer and microwave exposure until boiling. Slides were rinsed and treated with blocking buffer (2.5% horse serum in PBS) and exposed overnight at 4°C to primary antibody (rabbit anti-5-HT antibody; Sigma S5545; 1:200) diluted in blocking buffer. Following treatment with secondary antibody (anti-rabbit antibody 594, Invitrogen A11037; 1:1000), slides were mounted using Diamond antifade mountant with DAPI (Invitrogen P36966).

### **Solutions and drugs**

High extracellular  $\text{K}^+$  solution (30 mM KCl) was made by equimolar substitution of NaCl for KCl. The following reagents and drugs were obtained from Sigma-Aldrich (Oakville, ON, Canada): L-lactate, pyruvate, nifedipine, and  $\alpha$ -cyano-4-hydroxycinnamate. The pH of the extracellular solution was kept constant at ~7.8 following lactate addition. For chemostimulation, the perfusion fluid was bubbled with  $\text{N}_2$  gas for hypoxia, and a 5%  $\text{CO}_2$ /95% air gas mixture for hypercapnia.

### **Statistics**

The “n” values reported throughout represent the number of culture dishes sampled, except where noted. Statistical analysis was done using a one-way ANOVA with Dunnett's T3 multiple comparisons test.

## **RESULTS AND DISCUSSION**

### **Identification of killifish NECs**

As expected from previous studies on other aquatic vertebrates (Coolidge et al., 2008; Jonz and Nurse, 2003; Regan et al., 2011; Saltys et al., 2006; Zachar and Jonz, 2012), killifish gill sections contained 5-HT-immunoreactive NECs located mainly in the distal filaments (Figs. 1A-E).

Enzymatic dissociation of killifish gill tissue yielded many isolated cells that attached to the culture surface after a few hours incubation at room temperature (e.g. Fig. 2B2). In order to identify NECs, we used functional assays since it is well established that fish NECs are polymodal receptors that respond to high  $K^+$  depolarizations and sense chemostimuli, e.g. low  $O_2$  (hypoxia), high  $CO_2$  (hypercapnia) and  $NH_3$ , via signaling pathways that lead to intracellular  $Ca^{2+}$  elevations and neurotransmitter release (Abdallah et al., 2015; Porteus et al., 2021; Zachar et al., 2017; Zhang et al., 2011). Similar procedures are also routinely used to identify and characterize their mammalian counterparts, such as arterial carotid and aortic body chemoreceptors (Piskuric and Nurse, 2012; Torres-Torrelo et al., 2021), as well as airway chemoreceptors or pulmonary neuroepithelial bodies (Livermore et al., 2015), that share a common endodermal origin with fish NECs (Hockman et al., 2017).

### **Lactate stimulates intracellular $Ca^{2+}$ elevations in chemosensitive NECs**

During random sampling of dissociated fura-2 loaded killifish gill cells (typically 20 -130 cells sampled/dish), we encountered a small subpopulation with the expected properties of NECs. The latter cells generated intracellular  $Ca^{2+}$  signals when exposed to either hypoxia (15-20 mmHg), hypercapnia (5%  $CO_2$ ), and/or high (30 mM)  $K^+$  (Figs. 2A,C). For characterization of lactate sensing in these cells, confirmation of NEC identity was based primarily on their sensitivity to high  $K^+$  and, in some cases, to both hypercapnia and high  $K^+$  (e.g. Fig. 2C,D). Over the course of these studies, we found that ~90% of cells that responded to high  $K^+$  also responded to hypercapnia (Fig. 2E), suggesting that the majority of  $K^+$ -responsive cells was chemosensitive. Interestingly, in many cases, lactate (5 or 10 mM) induced intracellular  $Ca^{2+}$  elevations in the *same* cells that responded to either high  $K^+$  alone (Figs. 2B1,B2), or both hypercapnia and high  $K^+$  (Fig. 2C). Summary data comparing the peak  $Ca^{2+}$  elevations in NECs exposed to lactate, hypercapnia, and high  $K^+$  are shown in Fig. 2D. Pooled data comparing the proportion of ‘chemosensitive’ (i.e. lactate and/or  $CO_2$  sensitive) NECs within the high  $K^+$ -responsive population are shown in Fig. 2E. These data indicate that gill NECs, with well-established  $CO_2$ -chemosensing properties (Abdallah et al., 2015; Qin et al., 2010), can also sense lactate.

### **Role of L-type Ca<sup>2+</sup> channels and monocarboxylic acid transporters in lactate sensing**

The terminal steps in lactate sensing by mammalian carotid body glomus cells involve membrane depolarization, voltage-gated Ca<sup>2+</sup> entry, and neurotransmitter release (Torres-Torrelo et al., 2021; Torres-Torrelo et al., 2018). As illustrated in Fig. 3A, the lactate-induced intracellular Ca<sup>2+</sup> response in NECs was reversibly inhibited by nifedipine (0.5 μM), a blocker of voltage-gated L-type Ca<sup>2+</sup> channels. Summary data showing the effects of lactate on the intracellular Ca<sup>2+</sup> responses before, during, and after nifedipine are shown in Fig. 3B. These data suggest that lactate induced membrane depolarization and activation of L-type Ca<sup>2+</sup> channels in NECs, similar to carotid body glomus cells.

To probe further into the initial steps of the lactate chemotransduction cascade we tested certain aspects of the model proposed for lactate sensing in carotid body glomus cells (Torres-Torrelo et al., 2021; Torres-Torrelo et al., 2018). According to this model, lactate is co-transported with protons via a family of monocarboxylic acid transporters (MCTs) into the cell where it is converted to pyruvate by the enzyme lactate dehydrogenase; this reaction leads to a rapid increase in the NADH/NAD<sup>+</sup> ratio, activation of cation channels, and membrane depolarization. Consistent with this model, glomus cells showed high expression of MCT2 and MCT4, and importantly, lactate sensing in those cells was inhibited by AR-C155858, a MCT1/2 blocker, and by pyruvate which competes with lactate for transport by MCTs (Torres-Torrelo et al., 2021; Torres-Torrelo et al., 2018).

In concert with the findings in glomus cells, we found that a non-specific MCT1/2/4 blocker, α-cyano-4-hydroxycinnamate (CHC; 300 μM) (Miranda-Goncalves et al., 2013), and non-physiological levels of pyruvate (5 mM) reversibly inhibited the lactate-induced Ca<sup>2+</sup> elevations in killifish NECs, as exemplified in Fig. 3C and 3E, respectively. Of note, pyruvate caused intracellular Ca<sup>2+</sup> elevations in NECs when applied alone (Fig. 3E,F). This is consistent with the stimulatory effects of comparable levels of pyruvate on catecholamine secretion observed in carotid body glomus cells and is likely the consequence of intracellular acidification coupled to membrane depolarization (Torres-Torrelo et al., 2021). Summary data for the effects of CHC and pyruvate on lactate sensing in NECs are shown in Figs. 3D and 3F respectively. These data support a key role of MCTs in the lactate sensing pathway in NECs, though their molecular identity needs further characterization. In this regard, it is noteworthy that in a recent single cell transcriptomic study, zebrafish gill NECs expressed *slc16a3*, the gene that encodes MCT4, at a

significantly higher level than other gill cell types (Pan et al., 2022). Thus, MCT4 may well play a central role in lactate sensing by NECs in the gills of water breathers.

In summary, this is the first study to demonstrate that fish gill NECs directly sense lactate within the physiological range of blood concentrations (5-10 mM) that are known to stimulate ventilation (Thomsen et al., 2019; Thomsen et al., 2017). Thus, lactate adds to a growing list of metabolic factors, including low O<sub>2</sub>, high CO<sub>2</sub>/H<sup>+</sup> and NH<sub>3</sub>, that trigger adaptive cardiorespiratory reflexes in aquatic vertebrates by directly stimulating gill NECs (Jonz et al., 2004; Qin et al., 2010; Zachar et al., 2017). The first step in lactate sensing appears to be its transport into NECs by MCTs, coupled to a signaling pathway that ultimately leads to membrane depolarization, Ca<sup>2+</sup> entry through voltage-gated L-type Ca<sup>2+</sup> channels, and neurotransmitter (5-HT) release. In this regard, the lactate sensing pathway in NECs mimics some of the features elaborated in much greater detail in carotid body glomus cells (Torres-Torrelo et al., 2021; Torres-Torrelo et al., 2018). In the latter study, lactate sensing occurred over a comparable dose range and was accompanied by cytoplasmic acidification which could contribute in part to glomus cell depolarization. Hence, a similar acidification may contribute to the magnitude of the intracellular Ca<sup>2+</sup> responses recorded in NECs in the present study. However, further studies are required to determine whether the lactate sensing pathway in gill NECs involves the generation of intracellular signals (e.g. NADH and reactive oxygen species, ROS) coupled to downstream targets such as membrane ion channels, as reported for their mammalian counterparts (Torres-Torrelo et al., 2021; Torres-Torrelo et al., 2018).

### **Acknowledgements**

The authors thank Dr. Graham Scott and members of his staff for providing and maintaining the killifish used in the present studies.

### **Data availability**

Data are available from the figshare digital repository: [10.6084/m9.figshare.21539178](https://doi.org/10.6084/m9.figshare.21539178)

### **Competing interests**

The authors declare no competing interests.

## Author contributions

E.M.L and C.A.N. conceived and designed the experiments and wrote the manuscript. E.M.L and F.E.W. performed the experiments. All authors have reviewed and approved the final version of the manuscript.

## Funding

E.M.L. was supported by a Postdoctoral Fellowship from the Natural Sciences and Engineering Research Council of Canada (NSERC). This work was supported by grants to C.A.N. from NSERC (04464) and the Canadian Institutes of Health Research (MOP 142469).

## References

- Abdallah, S. J., Jonz, M. G. and Perry, S. F.** (2015). Extracellular H<sup>+</sup> induces Ca<sup>2+</sup> signals in respiratory chemoreceptors of zebrafish. *Pflugers Arch* **467**, 399-413.
- Borowiec, B. G. and Scott, G. R.** (2021). Rapid and reversible modulation of blood haemoglobin content during diel cycles of hypoxia in killifish (*Fundulus heteroclitus*). *Comp Biochem Physiol A Mol Integr Physiol* **261**, 111054.
- Brooks, G. A.** (2020). Lactate as a fulcrum of metabolism. *Redox Biol* **35**, 101454.
- Chang, A. J., Ortega, F. E., Riegler, J., Madison, D. V. and Krasnow, M. A.** (2015). Oxygen regulation of breathing through an olfactory receptor activated by lactate. *Nature* **527**, 240-4.
- Coolidge, E. H., Ciuhandu, C. S. and Milsom, W. K.** (2008). A comparative analysis of putative oxygen-sensing cells in the fish gill. *J Exp Biol* **211**, 1231-42.
- Gargaglioni, L. H., Bicego, K. C., Steiner, A. A. and Branco, L. G.** (2003). Lactate as a modulator of hypoxia-induced hyperventilation. *Respir Physiol Neurobiol* **138**, 37-44.
- Hardarson, T., Skarphedinsson, J. O. and Sveinsson, T.** (1998). Importance of the lactate anion in control of breathing. *J Appl Physiol (1985)* **84**, 411-6; discussion 409-10.
- Hockman, D., Burns, A. J., Schlosser, G., Gates, K. P., Jevans, B., Mongera, A., Fisher, S., Unlu, G., Knapik, E. W., Kaufman, C. K. et al.** (2017). Evolution of the hypoxia-sensitive cells involved in amniote respiratory reflexes. *Elife* **6**.
- Hui, S., Ghergurovich, J. M., Morscher, R. J., Jang, C., Teng, X., Lu, W., Esparza, L. A., Reya, T., Le, Z., Yanxiang Guo, J. et al.** (2017). Glucose feeds the TCA cycle via circulating lactate. *Nature* **551**, 115-118.
- Jonz, M. G., Fearon, I. M. and Nurse, C. A.** (2004). Neuroepithelial oxygen chemoreceptors of the zebrafish gill. *J Physiol* **560**, 737-52.
- Jonz, M. G. and Nurse, C. A.** (2003). Neuroepithelial cells and associated innervation of the zebrafish gill: a confocal immunofluorescence study. *J Comp Neurol* **461**, 1-17.
- Kumar, P. and Prabhakar, N. R.** (2012). Peripheral chemoreceptors: function and plasticity of the carotid body. *Compr Physiol* **2**, 141-219.



**Leonard, E. M. and Nurse, C. A.** (2020). Expanding Role of Dopaminergic Inhibition in Hypercapnic Responses of Cultured Rat Carotid Body Cells: Involvement of Type II Glial Cells. *Int J Mol Sci* **21**.

**Livermore, S., Zhou, Y., Pan, J., Yeger, H., Nurse, C. A. and Cutz, E.** (2015). Pulmonary neuroepithelial bodies are polymodal airway sensors: evidence for CO<sub>2</sub>/H<sup>+</sup> sensing. *Am J Physiol Lung Cell Mol Physiol* **308**, L807-15.

**Miranda-Goncalves, V., Honavar, M., Pinheiro, C., Martinho, O., Pires, M. M., Cordeiro, M., Bebiano, G., Costa, P., Palmeirim, I., Reis, R. M. et al.** (2013). Monocarboxylate transporters (MCTs) in gliomas: expression and exploitation as therapeutic targets. *Neuro Oncol* **15**, 172-88.

**Pan, W., Godoy, R. S., Cook, D. P., Scott, A. L., Nurse, C. A. and Jonz, M. G.** (2022). Single-cell transcriptomic analysis of neuroepithelial cells and other cell types of the gills of zebrafish (*Danio rerio*) exposed to hypoxia. *Sci Rep* **12**, 10144.

**Piskuric, N. A. and Nurse, C. A.** (2012). Effects of chemostimuli on [Ca<sup>2+</sup>]<sub>i</sub> responses of rat aortic body type I cells and endogenous local neurons: Comparison with carotid body cells. *J Physiol* **590**, 2121-2135.

**Porteus, C., Kumai, Y., Abdallah, S. J., Yew, H. M., Kwong, R. W. M., Pan, Y., Milsom, W. K. and Perry, S. F.** (2021). Respiratory responses to external ammonia in zebrafish (*Danio rerio*). *Comp Biochem Physiol A Mol Integr Physiol* **251**, 110822.

**Qin, Z., Lewis, J. E. and Perry, S. F.** (2010). Zebrafish (*Danio rerio*) gill neuroepithelial cells are sensitive chemoreceptors for environmental CO<sub>2</sub>. *J Physiol* **588**, 861-72.

**Regan, K. S., Jonz, M. G. and Wright, P. A.** (2011). Neuroepithelial cells and the hypoxia emersion response in the amphibious fish *Kryptolebias marmoratus*. *J Exp Biol* **214**, 2560-8.

**Saltys, H. A., Jonz, M. G. and Nurse, C. A.** (2006). Comparative study of gill neuroepithelial cells and their innervation in teleosts and *Xenopus* tadpoles. *Cell Tissue Res* **323**, 1-10.

**Thomsen, M. T., Lefevre, S., Nilsson, G. E., Wang, T. and Bayley, M.** (2019). Effects of lactate ions on the cardiorespiratory system in rainbow trout (*Oncorhynchus mykiss*). *Am J Physiol Regul Integr Comp Physiol* **316**, R607-R620.

**Thomsen, M. T., Wang, T., Milsom, W. K. and Bayley, M.** (2017). Lactate provides a strong pH-independent ventilatory signal in the facultative air-breathing teleost *Pangasianodon hypophthalmus*. *Sci Rep* **7**, 6378.

**Torres-Torrelo, H., Ortega-Saenz, P., Gao, L. and Lopez-Barneo, J.** (2021). Lactate sensing mechanisms in arterial chemoreceptor cells. *Nat Commun* **12**, 4166.

**Torres-Torrelo, H., Ortega-Saenz, P., Macias, D., Omura, M., Zhou, T., Matsunami, H., Johnson, R. S., Mombaerts, P. and Lopez-Barneo, J.** (2018). The role of Olfr78 in the breathing circuit of mice. *Nature* **561**, E33-E40.

**Zachar, P. C. and Jonz, M. G.** (2012). Neuroepithelial cells of the gill and their role in oxygen sensing. *Respir Physiol Neurobiol* **184**, 301-8.

**Zachar, P. C., Pan, W. and Jonz, M. G.** (2017). Characterization of ion channels and O<sub>2</sub> sensitivity in gill neuroepithelial cells of the anoxia-tolerant goldfish (*Carassius auratus*). *J Neurophysiol* **118**, 3014-3023.

**Zhang, L., Nurse, C. A., Jonz, M. G. and Wood, C. M.** (2011). Ammonia sensing by neuroepithelial cells and ventilatory responses to ammonia in rainbow trout. *J Exp Biol* **214**, 2678-89.

## Figures

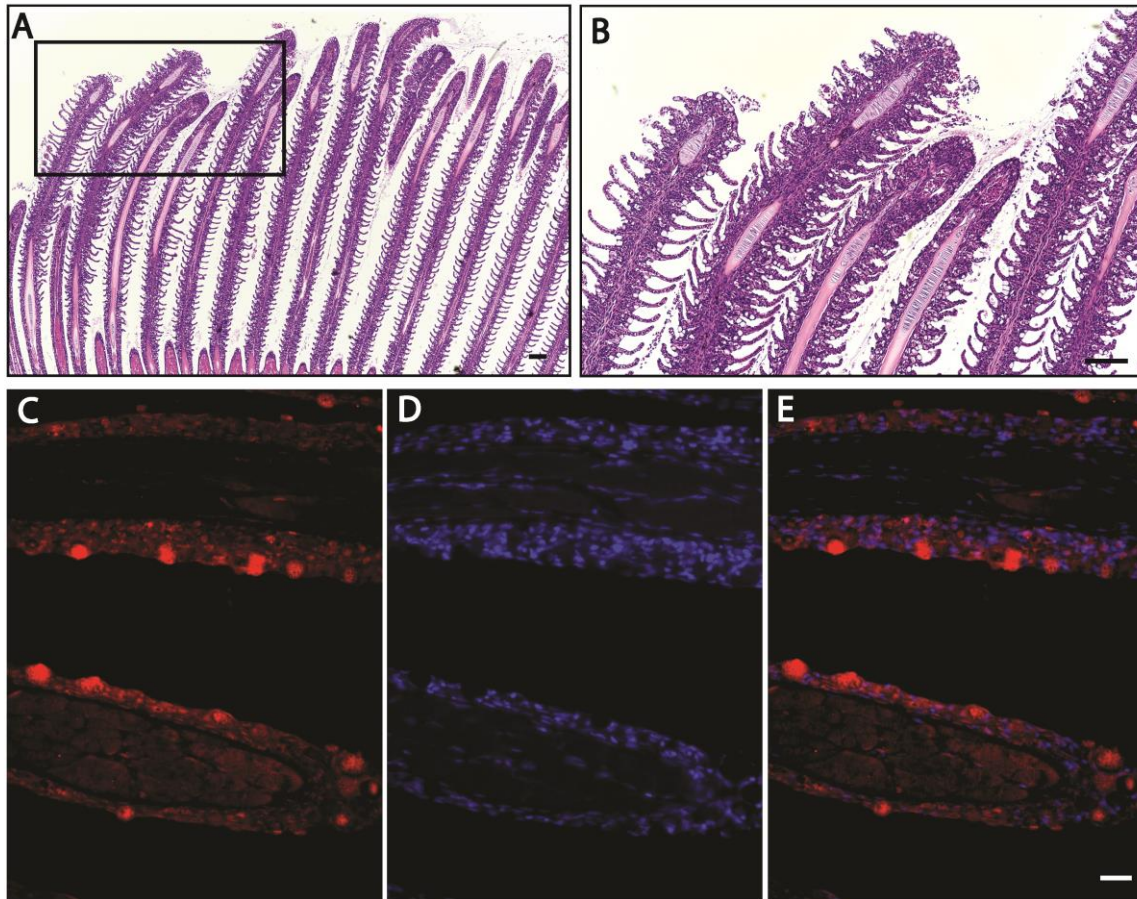


**Fig. 1. Killifish gill histology and 5-HT-immunofluorescence of NECs.** Example of H&E staining of a tissue section from killifish gill basket (A); rectangular region (A) is enlarged in B, showing the distal filaments and secondary lamellae. Scale bar for A and B: 100  $\mu\text{m}$ . C-E; section from a distal filament stained for 5-HT-immunofluorescence (red; C), DAPI (D), and merge (E). 5-HT-immunopositive NECs (red) are clearly visible in the two adjacent filament sections. In C-E, the section is oriented such that the distal side of the filament is located on the image right side, and the proximal side of the filament on the image left side. Scale bar C-E: 20  $\mu\text{m}$ .

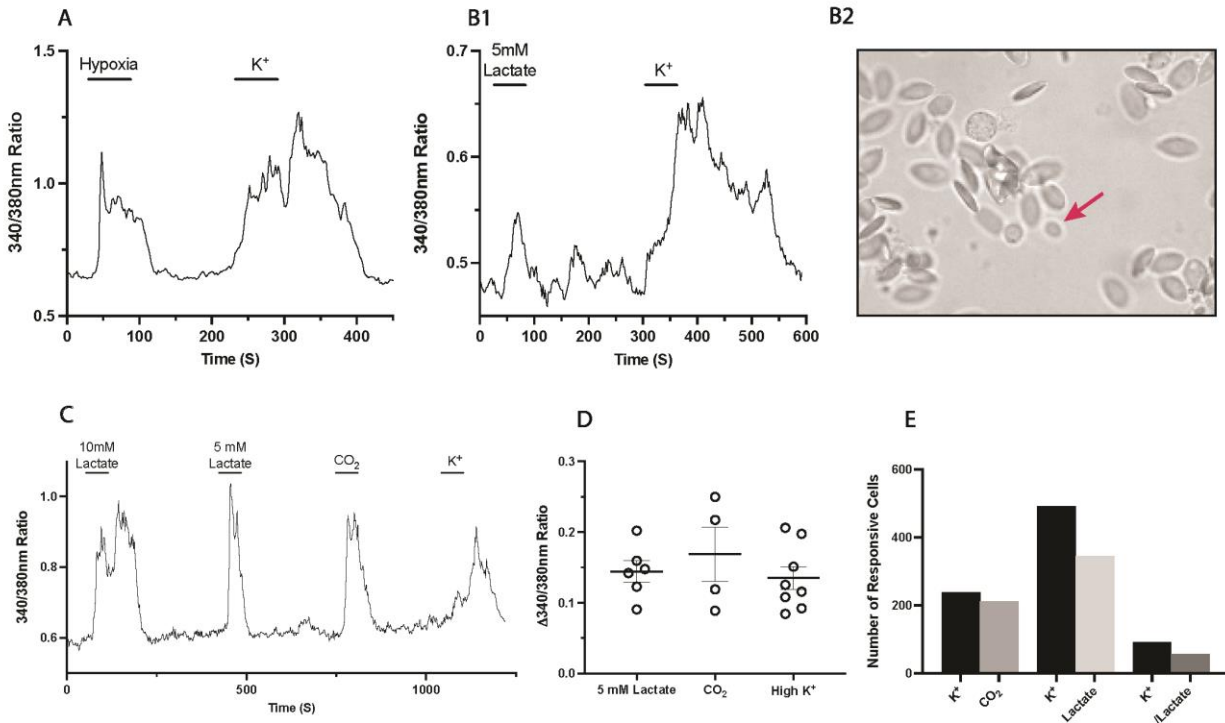


**Fig. 2. Lactate-induced intracellular  $\text{Ca}^{2+}$  elevations in functionally-identified killifish NECs.** An example of a NEC showing  $\text{Ca}^{2+}$  elevations during hypoxia and high (30 mM)  $\text{K}^{+}$  (A). In B1, a NEC labeled by the arrow in the micrograph (B2), responded to both lactate (5 mM) and high  $\text{K}^{+}$  with intracellular  $\text{Ca}^{2+}$  elevations. C; an example of a NEC that was equally sensitive to 5 and 10 mM lactate, as well as hypercapnia and high  $\text{K}^{+}$ . D; summary data of  $\text{Ca}^{2+}$  elevations in NECs exposed to 5 mM lactate, 5%  $\text{CO}_2$ , and high  $\text{K}^{+}$ ; each data point is the mean response from one fish. E; relative proportion of ‘chemosensitive’ (i.e. lactate and/or  $\text{CO}_2$  sensitive) NECs among the high  $\text{K}^{+}$  responsive cell population.

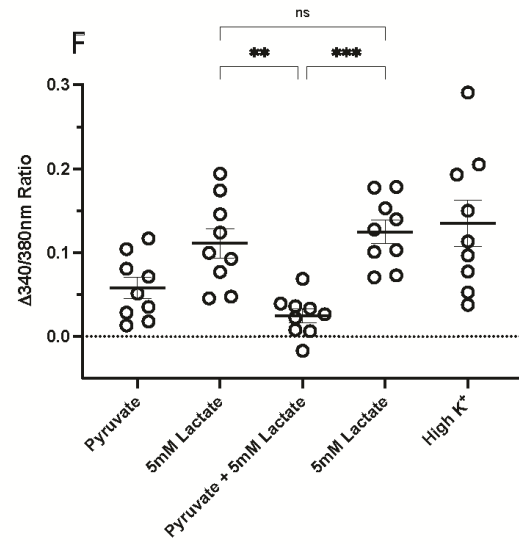
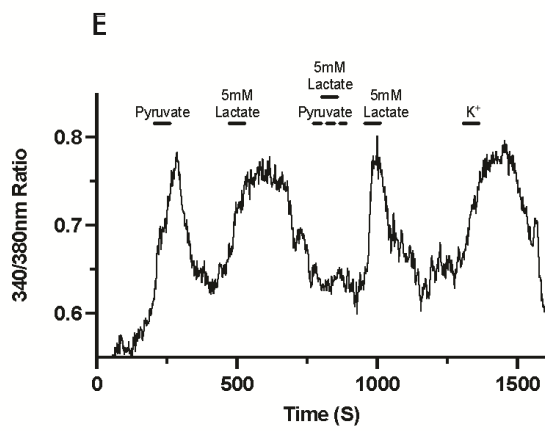
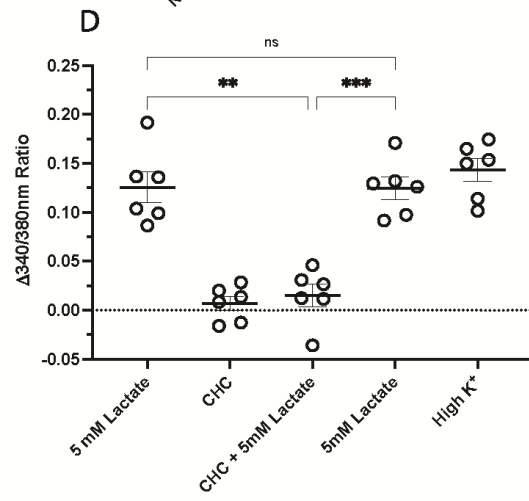
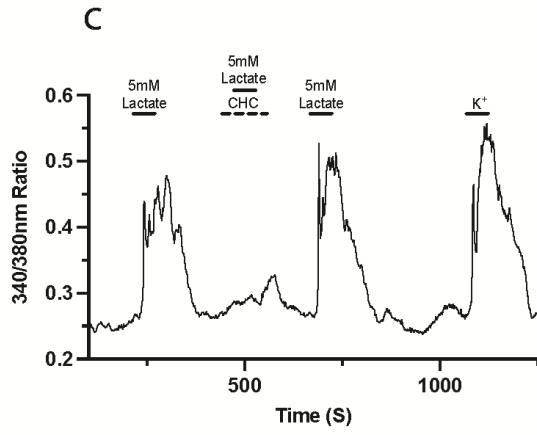
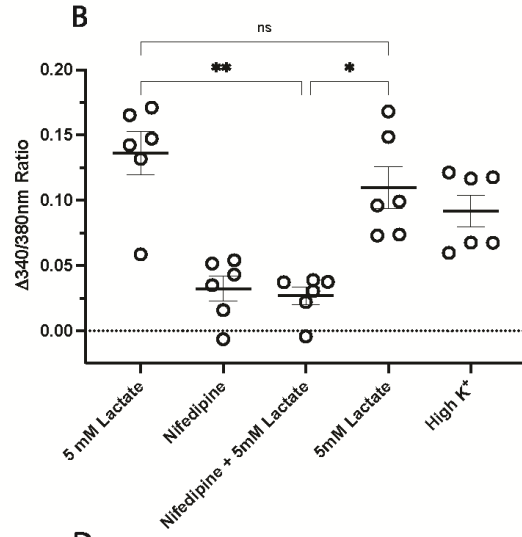
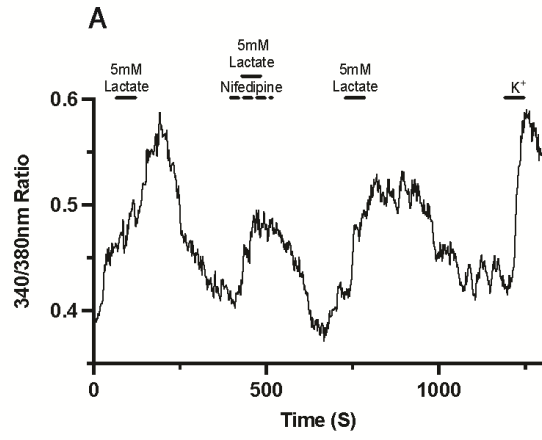


**Fig. 3. Role of voltage-gated  $\text{Ca}^{2+}$  channels and monocarboxylic acid transporters (MCTs) in NEC lactate sensing.** An example where the lactate-induced intracellular  $\text{Ca}^{2+}$  response in a NEC was reversibly inhibited by nifedipine (0.5  $\mu\text{M}$ ), a blocker of voltage-gated L-type  $\text{Ca}^{2+}$  channels (A). Summary data from 6 dishes treated in this way are shown in B, where each data point is the mean response from 4-10 cells in a single dish (# of fish =2). C; an example of the inhibition of lactate sensing in a NEC by  $\alpha$ -cyano-4-hydroxycinnamate (CHC; 300  $\mu\text{M}$ ), a non-specific MCT blocker; summary data from 6 dishes are shown in D (# of fish=2). In E, the NEC  $\text{Ca}^{2+}$  response induced by 5 mM lactate is reversibly inhibited by pyruvate (5 mM), which competes with lactate for MCTs; summary data from 9 dishes (# of fish =3) are shown in F. Note in E,F, that such ‘non-physiological’ levels of pyruvate induce intracellular  $\text{Ca}^{2+}$  responses in NECs when applied alone; this is likely a consequence of intracellular acidification as described in carotid body glomus cells (Torres-Torrelo et al., 2021). Significance levels are: \* $p < 0.05$ ; \*\*  $p < 0.005$ ; \*\*\*  $p < 0.0005$ .